Chirality

Deutsche Ausgabe: DOI: 10.1002/ange.201601156
Internationale Ausgabe: DOI: 10.1002/anie.201601156

Selective Dynamic Assembly of Disulfide Macrocyclic Helical Foldamers with Remote Communication of Handedness

*Christos Tsiamantas, Xavier de Hatten, Céline Douat, Brice Kauffmann, Victor Maurizot, Hirotaka Ihara, Makoto Takafuji, Nils Metzler-Nolte, and Ivan Huc**

Abstract: *Disulfide bridge formation was investigated in helical aromatic oligoamide foldamers. Depending on the position of thiol-bearing side chains, exclusive intramolecular or intermolecular disulfide bridging may occur. The two processes are capable of self-sorting, presumably by dynamic exchange. Quantitative assessment of helix handedness inversion rates showed that bridging stabilizes the folded structures. Intermolecular disulfide bridging serendipitously yielded a well-defined, C_2-symmetrical, two-helix bundle-like macrocyclic structure in which complete control over relative handedness, that is, helix–helix handedness communication, is mediated remotely by the disulfide bridged side chains in the absence of contacts between helices. MM calculations suggest that this phenomenon is specific to a given side chain length and requires disulfide functions*

Macrocyclization is a common approach to restrict the conformations available to an otherwise flexible molecular structure. It has broad significance in folded structures regardless of their size and complexity. In proteins, macrocyclization through disulfide bridges between cysteine residues far apart in the primary sequence stabilizes folded conformations, often via a destabilization of unfolded states, and contributes to resistance against proteolytic degradation.[1] Besides their frequent natural occurrence, protein disulfide bridges may also be engineered.[2] In essence, disulfide bridges couple the folding behavior of remote secondary motifs. These principles have been exploited at a smaller scale in synthetic objects, for example in the disulfide stabilization of α-helical peptides[3] and the capture of one handedness from a *P*-*M* mixture of 3_{10} helices.[4] Extensions of this concept include various stapling methods between amino acid side chains with chemical functions other than disulfides.[5]

Another important aspect of disulfide bridges is their ability to undergo thiol–disulfide exchange reactions.[6] In proteins, exchange reactions are critical to correct mismatched bridges when more than two cysteine residues are available. Thiol–disulfide exchange has also emerged as a powerful method for the dynamic covalent assembly of macrocycles from several dithiol units.[7,8] The formation of a particular macrocycle then reflects its intrinsic stability and the preorganization of the dithiol precursor for cyclization. Herein we report the first implementation of these principles in abiotic foldamer architectures. Depending on the positions of thiol-bearing side chains on aromatic oligoamide helical foldamers, we observed intra- or intermolecular dynamic disulfide formation with high selectivity, yielding large, structurally well-defined, macrocycles with a considerable and quantifiable stabilization of the folded conformations. Intermolecular bridging serendipitously produced a two-helix bundle-like structure with a unique, remote, helix-handedness communication mediated by disulfide-bridged side chains. This macrocycle consistently folds with the two helices having the same handedness even though there is no contact between them other than through the bridges. It provides an original example of long-range conformational coupling that could be useful in synthetic molecular-signaling systems and also a powerful tool to design elaborate multi-helical, tertiary-like abiotic architectures.

Oligoamides of 8-amino-2-quinolinecarboxylic acid adopt helical conformations that have been characterized in solution and in the solid state.[9] Helix stability increases with oligomer length, but folding remains dynamic; *P* and *M* conformations interconvert, the rate of handedness interconversion giving a quantitative measure of helix stability.[9c,d,10] In addition, helix stability can be modulated upon introducing units isosteric to, yet more flexible than, quinoline amino acids as well as various aliphatic monomers.[11] Aromatic oligoamide helices are thus robust and well suited to serve as components of larger architectures composed of several helical segments mimicking the super-secondary or tertiary structures of proteins.[12]

[*] Dr. C. Tsiamantas, Dr. X. de Hatten, Dr. C. Douat, Dr. V. Maurizot, Dr. I. Huc
University of Bordeaux, CBMN (UMR 5248)
Institut Européen de Chimie et Biologie
2 rue Escarpit, 33600 Pessac (France)
and
CNRS, CBMN (UMR 5248) (France)
E-mail: i.huc@iecb.u-bordeaux.fr
Dr. B. Kauffmann
University of Bordeaux, Institut Européen de Chimie et Biologie (UMS3033), 2 rue Escarpit, 33600 Pessac (France)
and
CNRS, IECB (UMS 3033), Pessac (France)
and
INSERM, IECB (US 001), Pessac (France)
Prof. H. Ihara, Dr. M. Takafuji
Kumamoto University, Department of Applied Chemistry and Biochemistry
2-39-1 Kurokami, Kumamoto 860-8555 (Japan)
Prof. N. Metzler-Nolte
Ruhr University Bochum, Faculty for Chemistry and Biochemistry
Universitätstrasse 150, 44801 Bochum (Germany)
Supporting information and the ORCID identification number(s) for the author(s) of this article can be found under http://dx.doi.org/10.1002/anie.201601156.

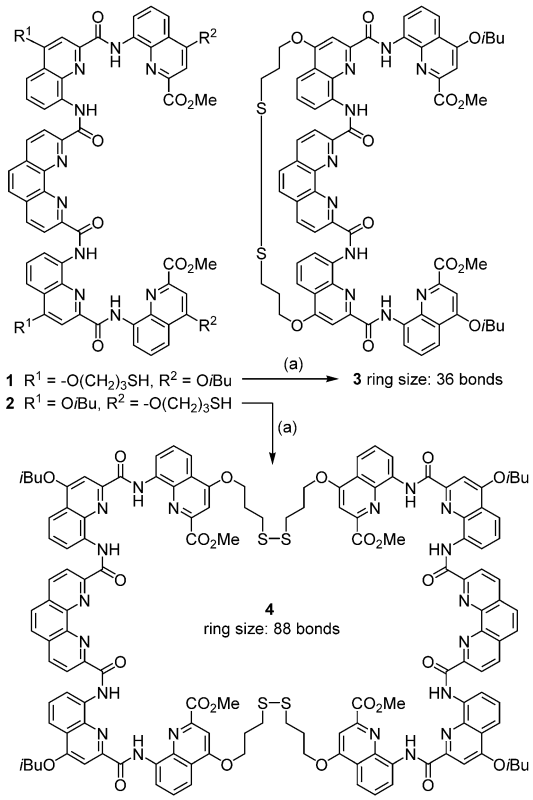

Scheme 1. Synthesis of macrocycles **3** and **4** from precursors **1** and **2**. Conditions: a) 14 mM in THF/H_2O (3:1 vol/vol), DIEA (40 μL), 25 °C, 48 h. DIEA = diisopropylethylamine.

Oligomers **1** and **2** (Scheme 1) were initially designed to explore whether disulfide bridges could be used to stabilize helical aromatic amide foldamers and assemble several helices together. The synthesis of **1** and **2** was carried out using established methods[13] (see Supporting Information). Both compounds bear two thiol functions that were protected as *tert*-butyl ethers during synthesis. The central phenanthroline unit[14] was introduced to make helices be C_2 symmetrical and avoid complications due to the $N\rightarrow C$ polarity that can result in parallel and antiparallel assemblies.

The crystal structure of the *tert*-butyl precursor of **1** (Figure 1 a) shows the expected helix structure spanning over two turns. Its two centrally located thiol-bearing chains are in close proximity and diverge from one side of the helix, hinting at the possibility of forming an intramolecular disulfide bridge. Indeed, exposure of **1** (14 mM in THF/H_2O, 3:1 vol/vol) to air in the presence of base leads to quantitative formation of intrastrand disulfide-bridged helix **3** (see Figure 1 b for model structure of **3**). High dilution is not required for this reaction. Evidence of the product structure comes from mass spectrometry, which shows a loss of two protons as compared to **1** (Figure S1 in the Supporting Information), and from ^{1}H NMR spectroscopy, which shows a deshielding ($\Delta\delta$ = 0.29 ppm) of the diastereotopic CH_2 protons geminal to the sulfur atom, along with an increased anisochronicity ($\Delta\delta$ = 0.22 ppm in **3** and close to 0 ppm in **1**, Figure 2 b). A crystal structure of **3** could not be obtained but the energy minimized model shown in Figure 1 b provides a realistic illustration of

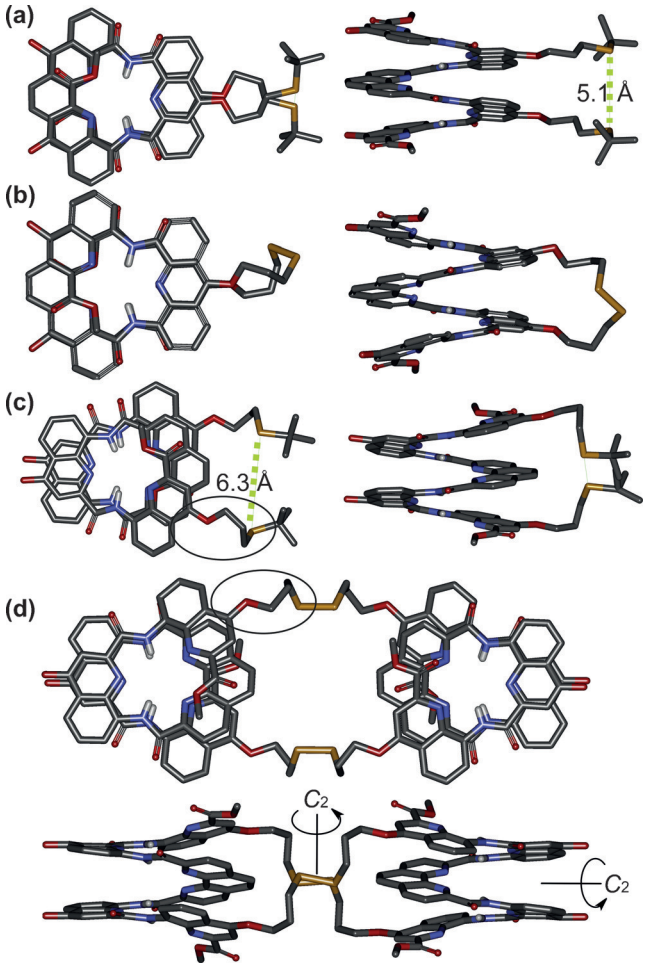

Figure 1. Crystal structures of the *tert*-butyl-protected precursors of **1** (a) and **2** (c) and crystal structure of **4** (d). Energy minimized (Maestro version 6.5 using the MM3 force field) conformation of the structure of **3** (b). In all cases, side views and top views are shown. Hydrogen atoms other than NH, included solvent molecules and isobutoxy side chains have been omitted for clarity. Ellipses denote similar side chain conformations in (d) and (c). C gray, S yellow, N blue, O red H white. Broken green lines indicate the selected interatomic distances.

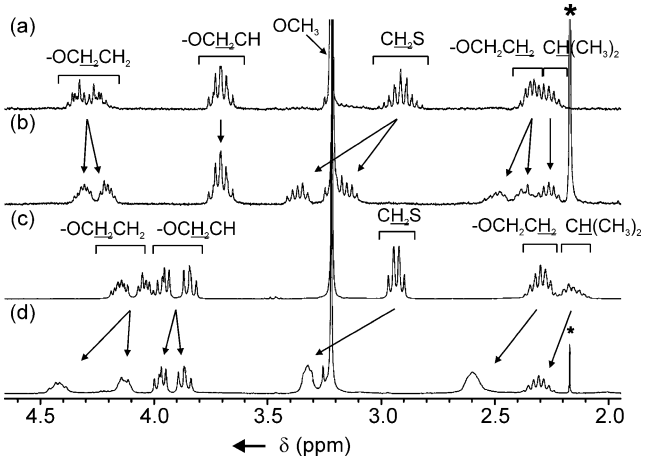

Figure 2. Part of the 300 MHz ^{1}H NMR spectra in $CDCl_3$ of compounds: a) **1**; b) **3**; c) **2**; and d) **4**. The star indicates residual acetone in the sample.

its cyclic folded conformation.[15] As a distinct element, all bonds of the side chains bearing the disulfide bridge adopt a *gauche* conformation, the disulfide bond itself having a dihedral angle close to 90°. The reaction was also carried out in $CHCl_3$/MeOH (80:20 vol/vol) for HPLC monitoring (Figure S3 a–c). The reaction proceeds smoothly at 5 mM. Decreasing the concentration to 1 and 0.2 mM slows down the reaction (see advancement after 48 h in Figure S3 a–c) which is not expected for an intramolecular reaction. This result suggests that intermolecular processes contribute to the faster reaction at 5 mM. Small amounts of a dimeric species are indeed detected resulting from intermolecular reactions, but these do not accumulate and presumably completely rearrange to form intramolecular disulfide bridged **3**. These species are not observed in the preparative scale conditions in THF/H_2O.

The crystal structure of the *tert*-butyl-protected precursor of **2** (Figure 1 c) shows that its thiol-bearing chains also protrude from the same side of the helix, but at distance too large to allow intrastrand disulfide bridge formation, even when taking into account side chain flexibility. Monte-Carlo conformational searches of a hypothetical intramolecular disulfide bridged derivative of **2** showed that the macrocycle accommodates an aromatic helix only with an increase of helix curvature (Figure S14) making this distorted species an unlikely product. Intramolecular disulfide bridge formation would require harsh conditions (e.g. 1M LiCl in NMP)[16] to destabilize the helix and was not investigated.

Experiments confirmed these predictions. The oxidation of **2** (14 mM in THF/H_2O, 3:1, vol/vol) produced the smallest accessible macrocycle, that is, interstrand disulfide-bridged dimer **4**, as a precipitate, in 71 % isolated yield, as confirmed by mass spectrometry and by GPC which shows that **4** is distinctly larger than **3** (Figures S2,S4). HPLC monitoring shows that the reaction is quantitative at 5 mM in $CHCl_3$/MeOH, a solvent where no precipitation occurs (Figure S3 f). Lowering concentration slows down the reaction. At 0.2 mM (initial conditions), the reaction is incomplete after 10 days; yet no other product formed in significant amounts (Figure S3 d), though it may be noted that normal phase HPLC did not allow to distinguish **4** from its mandatory non-cyclic precursor. The macrocyclizations of **1** and **2** are so selective that they proceed and self-sort in the same reaction flask. HPLC monitoring then shows the concomitant (and not subsequent, as would result from very different reaction rates) appearance of **3** and **4**. Under these conditions, intermolecular reactions of **2** occur to form **4** while **1** is present in the reaction medium. Thus, disulfide intermediates resulting from the reaction of **2** with **1** are likely as well but these eventually rearrange into **3** and **4**.

Dimer **4** can in principle exist as a mixture of *PP*, *MM*, and *PM* confomers.[12a,b] However, the presence of a single set of NMR signals suggested that one species prevailed (Figure 2 d, Figure S5). The chiral HPLC profile (Figure 3 c) indicated that the *PM* conformation is not populated. In agreement with this result, a crystal structure of **4** revealed a doubly C_2 symmetrical bundle of two helices having the same handedness (*PP* or *MM*) with their axes parallel (Figure 1 d). The dihedral angles at the disulfide bridges are near 90°.

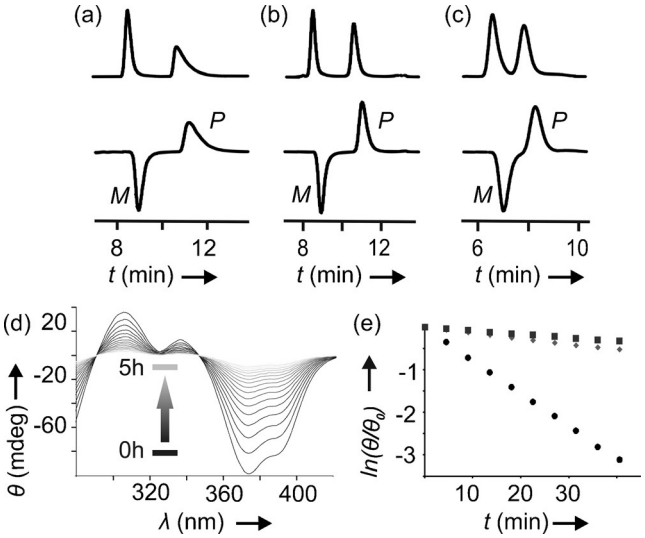

Figure 3. Helix racemization kinetics. Chromatographic separation (−5 °C, ChiralPack IA column, 5 μm particle size, 250×4.6 mm)) of *P* and *M* helices of: a) the *tert*-butyl-protected precursor of **1** (THF/Hexane, 40:60, vol/vol); b) **3** (THF/hexane, 50:50, vol/vol); and c) **4** ($CHCl_3$/AcOEt 30:70, vol/vol). UV detection traces (300 nm) are shown at the top, CD detector traces (360 nm) are shown at the bottom. d) Decay of the CD intensity over time of **4** in $CHCl_3$ at 30 °C. e) linear plots of CD intensity (381 nm) in $CHCl_3$ at 30 °C fitted to a first order decay for: **3** (◆), **4** (■), and the *tert*-butyl protected precursor of **1** (●).

Interestingly, as in the model of **3**, all methylene functions of the side chains are also involved in *gauche* conformations. In solution, the ^{1}H NMR spectrum of **4** features marked anisochronicity (up to $\Delta\delta = 0.3$ ppm) between diastereomeric protons of the sulfur bearing side chains (Figure 2 c,d). The quantitative (as far as NMR spectroscopy and HPLC can show) formation of the *PP*/*MM* conformer of **4** is remarkable in that there is no direct contact between the helices themselves. Unlike in other systems in which helix–helix side-by-side handedness communication was mediated by contacts between helices and was far from being quantitative,[12a,b,17] handedness is in this case communicated by the conformational preference of the connected 3-thiopropyloxy groups, a mechanism to be related with other remote chiral communication effects.[18,19]

To gain insights in this phenomenon, we carried out Monte-Carlo searches of preferred conformations (see Supporting Information). In the case of *PP*/*MM*-**4**, a unique stable conformer was found that accurately superimposes with the crystal structure, including at the disulfide bridges (Figure S11), thus hinting at a strongly preferred conformation of the whole macrocycle. In contrast, *PM*-**4**, a conformation that may exist as a transient species during the interconversion of the *PP* and *MM* conformations (see below), was found to adopt varied conformations of the macrocycle leading to multiple relative orientations of the helices (Figure S12). When the macrocycle of *PP*-**4** is theoretically cut open and one of the helices is removed, the energy minimized structure of that helix and two sulfide side-chains with their multiple *gauche* conformations perfectly overlaps with that of *PP*-**4** (Figure S13). This shows that

neither the aromatic helices nor the aliphatic bridges are strained in the macrocycle and that **2** happens to possess a geometry in which thiol functions are pre-oriented for macrocyclization as a *PP*/*MM* dimer. Indeed, the series of *gauche* conformations of the S–S bridged side chains in **4** is also seen in the *tert*-butyl-protected precursor of **2** (ellipses in Figures 1 c,d). Upon shortening each 3-thiopropyloxy group of **4** by one methylene unit, or upon replacing the S–S bridges by CH_2–CH_2 bridges, neither *PP*/*MM* nor *PM* macrocycles showed any marked preference for a particular conformation (Figures S15,S16). Specifically, the all-carbon bridges were found in multiple distinct conformations attempting to minimize the number of *gauche* conformations for both *PP*/*MM* and *PM* analogues (Figure S15). These calculations thus point at the unique behavior of *PP*/*MM*-**4**. Simple variants are predicted not to show a marked conformational preference.

Helix thermodynamic stability was quantitatively assessed for **3**, **4**, and the *tert*-butyl-protected precursors of **1** and **2** by measuring the rate of interconversion between *P* and *M* helices, a method that assumes that the activation energy required for this process reflects the energy difference between a folded ground state and an at least partly unfolded transition state.[9c,10] Conditions were first optimized to separate *P* and *M* helical conformers using chiral HPLC (Figure 3 a–c). A low eluent temperature (−5 °C) was maintained to reduce possible racemization on the column. In all cases, optimized HPLC profiles revealed a clean separation between an *M* helix eluting first (negative circular dichroism (CD) band at 360 nm)[20] and a *P* helix. Notably, in the case of **4**, no peak corresponding to a *PM* species was observed, in agreement with NMR data.

Fractions containing either *P* or *M* helices were collected after chiral HPLC separation and then evaporated at −5 °C to minimize racemization during this step. Racemization does not occur in the solid state and the evaporated samples can be stored for prolonged periods. After dissolving samples either in $CHCl_3$ or THF, the decay of specific bands in the CD spectra over time was recorded (Figure 3 d) and fitted to first order kinetics (Figure 3 e). Chromatograms of the equilibrated samples were identical to those observed prior to separation, confirming the absence of *PM*-**4**. The calculated half-lives of helix inversion are reported in Table 1. Non-bridged *tert*-butyl-protected precursors of **1** and **2** behave similarly, with half-lives of handedness inversion at 30 °C ranging from 4 min in $CHCl_3$ to 16 min in THF. In contrast, the half-lives of handedness inversion are about one order of magnitude larger for intrastrand disulfide-bridged helix **3**. Thus, macrocyclization enhances helix stability and validates the initial design. The half-life of helix handedness inversion of interstrand disulfide-bridged helix **4** in $CHCl_3$ is even larger than that of **3**. Again, disulfide-bridges bring about significant stabilization. In principle, the very large ring size of macrocycle **4** should make helix inversion easier than in **3**. However, it has to be considered that *PP*–*MM* handedness inversion in **4** spans not one but two helix segments that invert in a concerted manner, if not simultaneously. The *PM* intermediate, if it exists, quickly rearranges to a *PP* or *MM* conformer.

Table 1: Half-lives of helix inversion at 30 °C.

$t_{1/2}$ [min]	in $CHCl_3$	in THF
tert-butyl-protected precursor of **1**	4	16
tert-butyl-protected precursor of **2**	4	12
Compound **3**	53	150
Compound **4**	115	ND[a]

[a] not determined because of poor solubility.

Acknowledgements

This work was supported by the European Union through Marie Curie actions (FP7-PEOPLE-2010-ITN-264645, DYNAMOL, pre-doctoral fellowships to C.T.) and by ANR-DFG joint project FOLDHYD (ME 1378/15-1 and ANR-14-CE35-0016). We thank Dr. K. Ziach and Dr. T. Charoenraks for assistance with HPLC measurements, and Ms. M. Oikonomou and Dr. A. Velders for assistance with NMR assignment.

Keywords: chirality · foldamers · macrocycles · remote conformational communication · thiol-disulfide exchange

How to cite: *Angew. Chem. Int. Ed.* **2016**, *55*, 6848–6852
Angew. Chem. **2016**, *128*, 6962–6966

[1] a) S. Cheek, S. S. Krishna, N. V. Grishin, *J. Mol. Biol.* **2006**, *359*, 215–237; b) W. J. Wedemeyer, E. Welker, M. Narayan, H. A. Scheraga, *Biochemistry* **2000**, *39*, 4207–4216; c) L. Zhang, C. P. Chou, M. Moo-Young, *Biotechnol. Adv.* **2011**, *29*, 923–929; d) K. Huang, N. C. Strynadka, V. D. Bernard, R. J. Peanasky, M. N. James, *Structure* **1994**, *2*, 679–689; e) M. Matsumura, B. W. Matthews, *Methods Enzymol.* **1991**, *202*, 336–355; f) Z.-Y. Guo, Y.-M. Feng, *Biol. Chem.* **2001**, *382*, 443–448.

[2] a) D. Saerens, K. Conrath, J. Govaert, S. Muyldermans, *J. Mol. Biol.* **2008**, *377*, 478–488; b) P. Pecher, U. Arnold, *Biophys. Chem.* **2009**, *141*, 21–28; c) Y. Li, X. Li, X. Zheng, L. Tang, W. Xu, M. Gonga, *Peptides* **2011**, *32*, 1400–1407; d) N. E. Zhou, C. M. Kay, R. S. Hodges, *Biochemistry* **1993**, *32*, 3178–3187.

[3] D. Y. Jackson, D. S. King, J. Chmielewski, S. Singh, P. G. Schultz, *J. Am. Chem. Soc.* **1991**, *113*, 9391–9400; A. J. Nicoll, C. J. Weston, C. Cureton, C. Ludwig, F. Dancea, N. Spencer, U. L. Günther, O. S. Smart, R. K. Allemann, *Org. Biomol. Chem.* **2005**, *3*, 4310–4315; A. J. Nicoll, D. J. Miller, K. Fütterer, R. Ravelli, R. K. Allemann, *J. Am. Chem. Soc.* **2006**, *128*, 9187–9193; S. E. Miller, N. R. Kallenbach, P. S. Arora, *Tetrahedron* **2012**, *68*, 4434–4437; T. M. Postma, F. Albericio, *Eur. J. Org. Chem.* **2014**, 3519–3530.

[4] N. Ousaka, T. Sato, R. J. Kuroda, *J. Am. Chem. Soc.* **2009**, *131*, 3820–3821.

[5] A. M. Spokoyny, Y. Zou, J. J. Ling, H. Yu, Y.-S. Lin, B. L. Pentelute, *J. Am. Chem. Soc.* **2013**, *135*, 5946–5949; N. Ousaka, N. Tani, R. Sekiya, R. Kuroda, *Chem. Commun.* **2008**, 2894–2896; N. Ousaka, T. Sato, R. Kuroda, *J. Am. Chem. Soc.* **2008**, *130*, 463–465; C. E. Schafmeister, J. Po, G. L. Verdine, *J. Am. Chem. Soc.* **2000**, *122*, 5891–5892; J. Liu, D. Wang, Q. Zheng, M. Lu, P. S. Arora, *J. Am. Chem. Soc.* **2008**, *130*, 4334–4337; K. Fujimoto, M. Kajino, M. Inouye, *Chem. Eur. J.* **2008**, *14*, 857–863; Y. H. Lau, P. de Andrade, Y. Wu, D. R. Spring, *Chem. Soc. Rev.* **2015**, *44*, 91–102.

[6] P. A. Fernandes, M. J. Ramos, *Chem. Eur. J.* **2004**, *10*, 257–266.

[7] S. Otto, R. L. E. Furlan, J. K. M. Sanders, *J. Am. Chem. Soc.* **2000**, *122*, 12063 – 12064; S. Hamieh, V. Saggiomo, P. Nowak, E. Mattia, R. F. Ludlow, S. Otto, *Angew. Chem. Int. Ed.* **2013**, *52*, 12368 – 12372; *Angew. Chem.* **2013**, *125*, 12594 – 12598; S. Otto, R. L. E. Furlan, J. K. M. Sanders, *Science* **2002**, *297*, 590 – 593; J. M. A. Carnall, C. A. Waudby, A. M. Belenguer, M. C. A. Stuart, J. J.-P. Peyralans, S. Otto, *Science* **2010**, *327*, 1502 – 1506; K. R. West, K. D. Bake, S. Otto, *Org. Lett.* **2005**, *7*, 2615 – 2618.

[8] M. Li, K. Yamato, J. S. Ferguson, K. K. Singarapu, T. Szyperski, B. Gong, *J. Am. Chem. Soc.* **2008**, *130*, 491 – 500; J. Atcher, A. Moure, J. Bujons, I. Alfonso, *Chem. Eur. J.* **2015**, *21*, 6869 – 6878.

[9] a) H. Jiang, J.-M. Léger, I. Huc, *J. Am. Chem. Soc.* **2003**, *125*, 3448 – 3449; b) C. Dolain, A. Grélard, M. Laguerre, H. Jiang, V. Maurizot, I. Huc, *Chem. Eur. J.* **2005**, *11*, 6135 – 6144; c) N. Delsuc, T. Kawanami, J. Lefeuvre, A. Shundo, H. Ihara, M. Takafuji, I. Huc, *ChemPhysChem* **2008**, *9*, 1882 – 1890; d) T. Qi, V. Maurizot, H. Noguchi, T. Charoenraks, B. Kauffmann, M. Takafuji, H. Ihara, I. Huc, *Chem. Commun.* **2012**, *48*, 6337 – 6339.

[10] A. M. Abramyan, Z. Liu, V. Pophristic, *Chem. Commun.* **2016**, *52*, 669 – 672.

[11] D. Sánchez-García, B. Kauffmann, T. Kawanami, H. Ihara, M. Takafuji, M.-H. Delville, I. Huc, *J. Am. Chem. Soc.* **2009**, *131*, 8642 – 8648; M. Kudo, V. Maurizot, B. Kauffmann, A. Tanatani, I. Huc, *J. Am. Chem. Soc.* **2013**, *135*, 9628 – 9631; N. Delsuc, L. Poniman, J.-M. Léger, I. Huc, *Tetrahedron* **2012**, *68*, 4464 – 4469.

[12] a) N. Delsuc, J.-M. Léger, S. Massip, I. Huc, *Angew. Chem. Int. Ed.* **2007**, *46*, 214 – 217; *Angew. Chem.* **2007**, *119*, 218 – 221; b) N. Delsuc, S. Massip, J.-M. Léger, B. Kauffmann, I. Huc, *J. Am. Chem. Soc.* **2011**, *133*, 3165 – 3172; c) V. Maurizot, C. Dolain, Y. Leydet, J.-M. Léger, P. Guionneau, I. Huc, *J. Am. Chem. Soc.* **2004**, *126*, 10049 – 10052; d) N. Delsuc, M. Hutin, V. E. Campbell, B. Kauffmann, J. R. Nitschke, I. Huc, *Chem. Eur. J.* **2008**, *14*, 7140 – 7143; e) H.-Y. Hu, J.-F. Xiang, Y. Yang, C.-F. Chen, *Org. Lett.* **2008**, *10*, 69 – 72.

[13] T. Qi, T. Deschrijver, I. Huc, *Nat. Protoc.* **2013**, *8*, 693 – 708.

[14] For related foldamers based on 1,8-phenanthroline-2,7-dicarboxylic acid, see: Z.-Q. Hu, H.-Y. Hu, C.-F. Chen, *J. Org. Chem.* **2006**, *71*, 1131 – 1138.

[15] For related though less-well-defined structures, see: H. Abe, F. Kayamori, M. Inouye, *Chem. Eur. J.* **2015**, *21*, 9405 – 9413; S. Hecht, A. Khan, *Angew. Chem. Int. Ed.* **2003**, *42*, 6021 – 6024; *Angew. Chem.* **2003**, *115*, 6203 – 6206.

[16] H. Jiang, J.-M. Léger, P. Guionneau, I. Huc, *Org. Lett.* **2004**, *6*, 2985 – 2988.

[17] For another example of helix side-by-side handedness communication see: K. Maeda, M. Ishikawa, E. Yashima, *J. Am. Chem. Soc.* **2004**, *126*, 15161 – 15166.

[18] R. A. Brown, V. Diemer, S. J. Webb, J. Clayden, *Nat. Chem.* **2013**, *5*, 853 – 860; J. Clayden, A. Lund, L. Vallverdú, M. Helliwell, *Nature* **2004**, *431*, 966 – 971.

[19] Note added in proofs. Entropy was previously proposed as the reason of the higher stability of symmetrical homochiral macrocycles but we did not need to invoke such arguments here:S. W. Sisco, J. S. Moore, *Chem. Sci.* **2014**, *5*, 81 – 85.

[20] A. M. Kendhale, L. Poniman, Z. Dong, K. Laxmi-Reddy, B. Kauffmann, Y. Ferrand, I. Huc, *J. Org. Chem.* **2011**, *76*, 195 – 200.

Received: February 1, 2016
Published online: April 21, 2016

